



HAL
open science

Fluorescent Dyes as Partitioning Tracers for the Estimation of NAPL-Mass Saturation in Porous Media

Sofia Visitacion-carrillo, Stéfan Colombano, Nicolas Fatin-Rouge, Dorian Davarzani

► **To cite this version:**

Sofia Visitacion-carrillo, Stéfan Colombano, Nicolas Fatin-Rouge, Dorian Davarzani. Fluorescent Dyes as Partitioning Tracers for the Estimation of NAPL-Mass Saturation in Porous Media. *Ground Water Monitoring and Remediation*, 2023, 10.1111/gwmr.12591 . hal-04142019

HAL Id: hal-04142019

<https://brgm.hal.science/hal-04142019>

Submitted on 26 Jun 2023

HAL is a multi-disciplinary open access archive for the deposit and dissemination of scientific research documents, whether they are published or not. The documents may come from teaching and research institutions in France or abroad, or from public or private research centers.

L'archive ouverte pluridisciplinaire **HAL**, est destinée au dépôt et à la diffusion de documents scientifiques de niveau recherche, publiés ou non, émanant des établissements d'enseignement et de recherche français ou étrangers, des laboratoires publics ou privés.



Distributed under a Creative Commons Attribution - NonCommercial - NoDerivatives 4.0 International License

Fluorescent Dyes as Partitioning Tracers for the Estimation of NAPL–Mass Saturation in Porous Media

by Sofia Visitacion-Carrillo, Stéfan Colombano, Nicolas Fatin-Rouge and Dorian Davarzani 

Abstract

Accurate estimation of the nonaqueous phase liquids (NAPLs) saturation such as chlorinated organic compounds (COCs) in aquifers is crucial for the proper remediation of contaminated groundwater. A combination of conservative and partitioning tracers (PTs) are commonly used to assess NAPL saturations in the subsurface at COC release sites, using the partitioning interwell tracer test (PITT). In this study, five fluorescent dyes were assessed as PTs to estimate the saturation of octanol and 3 COC NAPLs in soil columns. PT experiments required an initial assessment of both partitioning (NAPL/water and octanol/water) and linear free-energy relations. The predictability of the partition coefficients was correlated to the pH of the two-phase fluids for both systems (NAPL/water and octanol/water). The COC NAPLs were acidic and some PTs with acid-base properties, like fluorescein, are easily influenced by pH. The PITT experiments were performed in a column packed with glass beads, using rhodamine WT as PT because of its particular specificity for the complex mixture of NAPLs and sodium chloride as the inert tracer. Breakthrough curves of rhodamine WT were examined to estimate the saturation of a NAPL made of a complex mixture of COCs. The DNAPL residual saturation estimation accuracy was sensitive to both pH variations and the water velocity. The latter was represented by an exponential function which resulted from non-equilibrium measurements, heterogeneous sweeping of the contaminated sample, and redistribution of the NAPL droplets in the medium.

Introduction

Historical use of chlorinated organic compounds (COCs) has resulted in widespread contamination of soil and groundwater. According to the BASOL database (MTES 2018), chlorinated solvents are found in 17% of sites monitored by the French government. Moreover, 36% of the water resources used for drinking water supplies (domestic and public supply wells) are not in fact used due to contamination. In source zones, they are present as dense non-aqueous phase liquids (DNAPLs), which migrate vertically downward through aquifer systems, ultimately residing along low-permeability units such as aquitards and confining layers. The migration results in occurrence of residual

NAPL within the porous media that can serve as long-term source of COCs that pose a risk to human health if consumed via drinking water. Removal of DNAPLs through natural dissolution is estimated to take from decades to centuries (ITRC 2005). Thus, DNAPLs are a persistent threat to human health and the environment (NIEHS 2015).

The mass and shape of the source of pollution are closely linked to the size of plumes, which supports the use of source area treatment technologies in the early stages of remediation (DiFilippo and Brusseau 2008). Therefore, accurate conceptual site models that define shape, mass, saturation, and composition are critical for successful remediation. It is known in field experiments that a thorough understanding of the distribution of the NAPL can support more targeted, cost-effective remediation technologies compared to blind extraction techniques such as the well-known “pump and treat” method (Falta et al. 2005; McDade et al. 2005; McGuire et al. 2006).

Among the gamut of tools for estimating NAPL distribution and saturation, partitioning tracer (PT) tests can assess large volumes of contaminated material, the mass and the average saturation of NAPLs, and also extraction efficiency (Jin et al. 1995; Jin et al. 1997; Thal et al. 2007). Field application of a partitioning interwell tracer test (PITT) involves injecting two tracers (a conservative tracer is mixed with ones that partition) into the aquifer and uses the delay between these two tracer signals to estimate NAPL

Article impact statement: A unique method to predict the residual NAPL saturation of high velocity contaminated aquifers using fluorescent tracers.

© 2023 The Authors. *Groundwater Monitoring & Remediation* published by Wiley Periodicals LLC on behalf of National Ground Water Association. doi: 10.1111/gwmmr.12591

This is an open access article under the terms of the [Creative Commons Attribution-NonCommercial-NoDerivs](https://creativecommons.org/licenses/by-nc-nd/4.0/) License, which permits use and distribution in any medium, provided the original work is properly cited, the use is non-commercial and no modifications or adaptations are made.

quantity. Typically, the PTs are alcohols ranging from propanol to octanol, which are injected into the aquifers at concentrations of tens of g/L (Jin et al. 1995; Jalbert et al. 2003; Hartog et al. 2010). The coupling of conservative and non-conservative tracers allows an accuracy of more than 20% in NAPL saturation estimates at the laboratory-scale for low permeability materials (Thal et al. 2007). By measuring tracers' concentration profiles with known partition constants we can deduce water volumes, while the lag time between the conservative tracer and the others provides the nonaqueous phase liquid (NAPL) saturation. Although PITT are usually performed under forced gradient conditions, their accuracy may be decreased in high-velocity aquifers (Ervin et al. 2011; Muller and Ramsburg 2018). In some cases, complexity in the alcohols' molecular structures makes it difficult to determine the partition coefficients between the NAPL and the tracer (Ghanem et al. 2003). Varying tracer properties with environmental conditions such as pH can be problematic (Klonis and Sawyer 1996). Moreover, the biodegradability of alcohol tracers may affect recovery and accurate characterization of the tail of the tracer breakthrough curves. Annable et al. (1998) noted the presence of degradation of the tracers ethanol, *n*-pentanol, and *n*-hexanol by 35%, 24%, and 39%, respectively, during their in situ experiments. Furthermore, surfactant properties (reducing the interfacial tension) are of concern since the uncontrolled downward migration, and then repositioning, of DNAPLs because of decreasing pores' entry capillary pressure (Rathfelder et al. 2003; Maire and Fatin-Rouge 2017). In some cases, gas-phase PT tests such as helium (Simon and Brusseau 2007), sulfur hexafluoride (Wilson and Mackay 1995), and chlorofluorocarbons (Chambers et al. 2019; Cook et al. 1995; Werner and Höhener 2002; Werner et al. 2009) were found to predict the residual saturation reasonably well. However, the physico-chemical environment (especially the organic matter content) can dictate a conservative or non-conservative tracer behavior. The sorption of tracers to soil organic matter leads to an increase in the retardation factor (*R*) and to an overestimation of NAPL saturation (Khan et al. 2008). Several studies have calculated the retardation factors (*R*) due to the adsorption of fluorescent tracers on organic matter (Vasudevan et al. 2001). Oba and Poulson (2012) demonstrated that *R* varied between 1.02 and 4.04 and 1.00 to 2.00 for Fluorescein and Eosin Y (at different pH), respectively. In the case where adsorption on mineral surfaces is not too high, the residual saturation calculations are more precise (Jin et al. 1995). For low NAPL residual saturations, tracers can be absorbed on the natural organic material and potentially increase the retardation factor (Jin et al. 1997).

Fluorophores are chemical compounds that can re-emit light upon excitation. These compounds have been used for decades for the characterization of high-velocity aquifers. These compounds have been successfully used at sub mg/L concentrations because of their high detection sensitivity and their intensity-concentration relation having a large linear range (Kasnavia et al. 1999; Dörflinger 2010). The PITT technique with fluorescent tracers is promising and is beginning to be used frequently in oilfield applications (Ohms et al. 2010; Król et al. 2021). However, their use for PT

applications may be tricky, for example, when complex speciation vs. pH occurs (Klonis and Sawyer 1996). Moreover, despite linear relations that have been observed for the partitioning of compounds between simple two-phase systems, actual field conditions are more complex, involving multiple phases (soil, NAPL, air, water), chemical mixtures, and other variable processes like biodegradation (Ervin et al. 2011).

Fluorescent tracers have several advantages: (1) their quantification limit is approximately 10^4 times lower than non-fluorescent tracers; (2) they are relatively inexpensive and nontoxic at low concentrations; (3) they can be analyzed on-site via simple, portable, and cost-efficient analytical techniques (i.e., UV-Vis spectroscopy, and digital color analysis) (Aparecida de Melo and de Holleben 2001; Khmel'nitskiy et al. 2022). They are used in oilfield applications (Ohms et al. 2010; Król et al. 2021).

The purpose of our study was, first, to study the applicability of fluorescent tracers for the estimation of NAPL saturations in a sedimentary aquifer, focusing on COC-contaminations with increasing chemical complexity. Second, we explored the validity of the linear relation for the partitioning of tracers between organic/water systems. Third, we demonstrated the effect of groundwater velocity on the DNAPL residual saturation estimation accuracy (RSEA) in a laboratory-scale experimental setup.

Properties of Tracers and Pollutants

Tracers

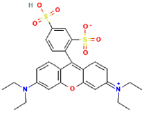

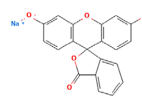
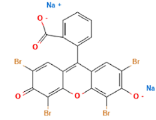
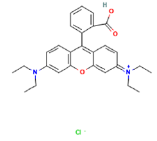
Five fluorophores were selected as potential PTs (see Table 1). Dye concentrations in water were analyzed by UV/Visible spectrophotometry rather than by fluorescence, since the latter is easily hindered by various mechanisms (Leibundgut et al. 2009). A Cary UV 60 spectrophotometer coupled with a Torlon® probe body (Agilent Technologies, Inc) was used for measurements. The Beer-Lambert law was checked for each compound through calibration curves carried out at the wavelength of maximum absorption.

Table 1 includes ranges of published $\log K_{ow}$ values for the fluorescent dyes selected for this study. While only one published data was registered for RWT $\log K_{ow}$ value, the other dyes presented a deviation of at least one log unit within the available literature ($F \gg EY > SRB > RB$). Any alteration in the measurement protocol of K_{ow} can drastically affect the effective comparison between studies (e.g., temperature, stability to degradation, pH, and the presence of an aqueous buffer) (Dearden and Bresnen 1988; Harris and Logan 2014; Cumming and Rucker 2017).

Two-Phase Liquid Systems

The PT distribution of the dyes was studied in two-phase liquid systems made of deionized water and a NAPL in contact, allowing the PT to distribute between them. The NAPLs (*N*) used in this study were: octanol (*O*), a historical DNAPL made of several COCs in a complex mixture (*M*), a one-COC (*H*), and a three-COCs (*T*) surrogate both based on the most abundant constituents in *M* (see Table 2). *M* was collected from a weathered COC release site in France, where a COC leak occurred in the late 1960s (Maire and Fatin-Rouge 2017). The DNAPL was a complex mixture

Table 1
Chemical Properties of the Fluorescent Dyes

Compound	SRB	RWT	F	EY	RB
Structure					
Formula	C ₂₇ H ₃₀ N ₂ O ₇ S ₂ Na ₂	C ₂₉ H ₂₉ Cl N ₂ Na ₂ O ₅	C ₂₀ H ₁₀ Na ₂ O ₅	C ₂₀ H ₁₂ Br ₄ Na ₂ O ₈	C ₂₈ H ₃₁ Cl N ₂ O ₃
λ _{max} ¹ (nm)	565	557	485	515	555
L.O.Q. ² (µg/L)	21	16	31	28	17
logK _{ow} ³	[-2.96; -0.45]	-1.33	[-4.77; 3.30]	[-1.27; 0.83]	[1; 2.49]
pKa	<1.5 ⁴	5.1 ⁴	2.2; 4.4; 6.7 ⁵	2.0; 3.8 ⁶	3.0 ⁴
Solubility in water (g/L) ⁴	70	180	25	>100	20
Provider	Sigma Aldrich	Acros Organics	Acros Organics	Fisher Scientific	Acros Organics

EY, eosin Y; F, fluorescein; SRB, sulfurhodamine B; RB, rhodamine B; RWT, rhodamine WT.

¹Maximum absorption wavelength.

²Limit of quantification in this study.

³Detailed information in Supplementary Material S1.

⁴Kasnavia et al. (1999).

⁵ChemicalBook (2022).

⁶Majek et al. (2014).

Table 2
Physicochemical Properties of the Chlorinated Compounds Used in this Study

Compounds	Molar Mass (g/mol)	Density (20°C) ¹	S (mg/L) ¹	logK _{ow} ¹	M		T		H
					% (w/w) ²	C (mg/L) ³	% (w/w)	C (mg/L) ³	S (mg/L)
Hexachlorobutadiene (HCBd)	261	1.68	3.23	4.78	55	1.38	71.6	2.02	3.23
Hexachloroethane (HCEa)	237	2.09	50	4.14	14	5.08	17.9	7.31	
Perchloroethylene (PCE)	166	1.62	206	3.40	8	19.42	10.5	28.70	
Pentachlorobenzene (PeCB)	250	1.83	499.5	0.419	4	28.18	—	—	
Tetrachloride carbon (TCM)	154	1.58	793.4	2.83	3	17.95	—	—	
Trichloroethylene (TCE)	131	1.46	1280	2.42	2	37.39	—	—	
Hexachlorobenzene (HCB)	285	2.05	0.005	5.44	1	0.00008	—	—	
Others					13	—	—	—	
Total effective aqueous solubility						109.40		38.03	3.23

S, solubility in water; C, estimated aqueous concentration.

¹Mackay and Cherry 2016; Montgomery 2007.

²Cazaux et al. 2014.

³Estimation of the solubilities based on the Banerjee equation (Banerjee 1984) and the UNIFAC method (UNIFAC Functional-group Activity Coefficients).

primarily of hexachlorobutadiene (HCBd), hexachloroethane (HCEa), and perchloroethylene (PCE). H (HCBd) and the T blend (mixture of HCBd, HCEa, and PCE) were prepared using pure laboratory supplies provided by Fischer Scientific. Octanol was used as a reference NAPL. The general composition and specifications of the substances used in this study are presented in Table 2.

Experimental Setup and Procedures

Partition of Dyes in Batch NAPL/Water Systems

The partition coefficients of the fluorescent dyes (F, EY, RB, SRB, and RWT) between the NAPL/water systems were calculated according to the OECD recommendations (OECD 1995). All experiments were performed in batches with deionized water, obtained from a Milli-Q water

system (18.2 M Ω cm) and degassed before use with an ultrasonic bath (Elmasonic P 120H, 80 kHz). Experiments were carried out in triplicate inside 30 mL airtight cylindrical glass reactors containing 20 mL aqueous solution of dye at concentrations of 0.5, 1, 2.5, 5, and 10 mg/L. Dye partition was initiated by adding 1 mL of NAPL to glass reactors stored in the dark at 20°C, with stirring (150 rpm). Partition was stopped after 24 h, then 10 mL aliquots were collected from the aqueous phase for measurement of dye concentration. Before and after the partition experiments, the pH was measured in the aqueous phase (see Supplementary Material S2). The pH was measured with a glass electrode (Radiometer Analytical pHC3005-8, Hach), which was calibrated before each experiment with commercial buffer solutions (pH 10, 7, and 4). Partition coefficients were calculated according to the following relation (Schwarzenbach et al. 2017):

$$K_{Nw} = \frac{C_N}{C_w} \quad (1)$$

where K_{Nw} is the partition coefficient of the dye between the NAPL (N) and the aqueous phase (w). C_N and C_w are the dye concentrations (M/L³) in each phase. C_N was calculated from the mass balances on dyes and based on C_w measurements using the Beer-Lambert law.

PT Tests in Column

When tracers with different partition coefficients (K_{Nw}) are injected into a contaminated aquifer under forced-gradient conditions, inert tracers remain in the aqueous phase and move at the injection flow rate, while the PTs have a delayed release because of their in the NAPL partitioning (Annable et al. 1998). The delayed PT release is characterized by a retardation factor, R , which is defined as:

$$R = \frac{\bar{t}_{PT}}{\bar{t}_{IT}} \quad (2)$$

where \bar{t}_{PT} and \bar{t}_{IT} [T] are the mean residence times of the PT and the inert tracer, respectively.

A column study was performed as a model of contaminated permeable unconsolidated material in which the fluorescent dyes were injected to assess the NAPL saturation, according to:

$$S_N + S_w = 1 \quad (3)$$

where S_N and S_w (dimensionless) are the average NAPL and water saturations, respectively.

The experimental setup used for the partitioning tests is presented in Figure 1. Glass beads of ~1 mm diameter were passed through sieves to ensure glass bead size tolerance of $\pm 4\%$ (960 and 1040 μ m mesh). The beads were then packed into a glass column (length: 10 cm, i.d.: 5 cm). Degassed water was injected into the system with a membrane pump (SIMDOS 10; KNzF Laboratories; 2% accuracy). Weight and volume measurements were performed to calculate the porosity of the media which was $38.9\% \pm 0.6\%$. Permeability of the porous media was measured experimentally according to Darcy's law by setting a hydrostatic height above the porous sample and measuring the water flow rate at its output following the same protocol as (Colombano

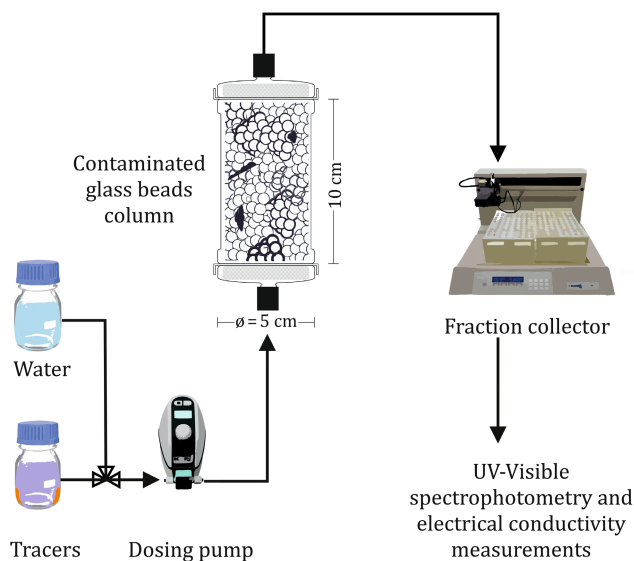


Figure 1. Experimental setup of the PT experiments.

et al. 2020, 2021; Philippe et al. 2020, 2021). The measured absolute permeability was 3.5×10^{-10} m². The porosity and permeability values measured in this study are very close to the ones reported in the literatures (Philippe et al. 2020, 2021; Cochenne et al. 2022) using the same glass beads.

The experiments were performed with the historical complex DNAPL (M). Residual saturation of M inside the column of porous material was achieved in two steps. First, by carefully injecting 1 PV of M in a flow rate of 1 mL/min in the ascending direction. Then, 10 pore volumes (PV) of degassed water were injected from the top of the column at higher flow rates, while M was recovered at its bottom. The effluent was directed to a phase separator to measure the amount of M recovered as a pure phase. The residual saturation achieved in these experiments was $2.48 \pm 0.21\%$. We chose these initial conditions for the experiments because the method's accuracy requires a homogeneous sweeping of the contaminated material. Working with residual saturation increases the accuracy of the results by preventing DNAPL pools. The irregularly distributed hydrocarbon saturation and presence of free-phase NAPL can decrease the accuracy of the standard method of moments. (Jin et al. 1997; Salman and Kostarelos 2019).

PT tests were performed by injecting 0.36 PV of tracers (RWT at 10 mg/L mixed with 0.01 M NaCl) at flow rates of $q = 1, 4, 10,$ and 40 mL/min (1.9, 7.5, 18.8, and 75.2 m/d, respectively). RWT and sodium chloride were used as PT and inert tracer, respectively. Before the experiments, we confirmed that the RWT does not adsorb onto the glass beads. At least three PV of degassed water were injected after the introduction of tracers. The tracers were monitored from the beginning of tracer injection in the water effluent at the output of the column. Aliquots of 4 mL of water effluent samples were collected periodically until the tracers were no longer detected. Each effluent sample was analyzed for conductivity and RWT concentration from light-absorption at 557 nm.

Response curves for tracer recovery were analyzed using the method of moments (Jin et al. 1995; Jalbert et al. 2003).

Table 3**Partition Coefficients of Fluorescent Dyes**

System	pH	$\log K_{Nw}$	SRB	RWT	F	EY	RB
O,W	5.92±0.42	$\log K_{ow}$	-0.110±0.04	-0.369±0.039	0.905±0.039	0.084±0.084	1.881±0.014
		R ²	0.975	0.976	0.984	0.899	0.997
H,W	5.10±0.37	$\log K_{hw}$	-0.011±0.032	-0.349±0.027	1.022±0.015	0.164±0.044	1.700±0.015
		R ²	0.984	0.989	0.998	0.970	0.996
T,W	4.39±0.18	$\log K_{tw}$	-0.085±0.068	-0.048±0.014	1.663±0.035	1.419±0.038	1.843±0.023
		R ²	0.931	0.997	0.987	0.998	0.991
M,W	4.21±0.20	$\log K_{mw}$	-0.016±0.105	1.022±0.028	1.856±0.024	2.296±0.018	2.610±0.028
		R ²	0.850	0.987	0.994	0.995	0.988

EY, eosin Y; F, fluorescein; SRB, sulforhodamine B; RB, rhodamine B; RWT, rhodamine WT; O, octanol; W, water; H, hexachlorobutadiene; T, three-component NAPL mixture; M, complex NAPL mixture.

Assuming the PT reaches the equilibrium between the two liquid phases, the residual saturation of the NAPL in the porous media is obtained from:

$$S_x = \frac{\bar{t}_{PT} - \bar{t}_{IT}}{(K_{Nw} - 1)\bar{t}_{IT} + \bar{t}_{PT}} \quad (4)$$

where the partition constant K_{Nw} for RWT was obtained from experiments in the two-phase liquid system, and where \bar{t}_{PT} and \bar{t}_{IT} are calculated from:

$$\bar{t}_{PT} = \frac{\int_0^{t_s} t C_{PT}(t) dt}{\int_0^{t_s} C_{PT}(t) dt} - \frac{t_s}{2} \quad (5)$$

$$\bar{t}_{IT} = \frac{\int_0^{t_s} t C_{IT}(t) dt}{\int_0^{t_s} C_{IT}(t) dt} - \frac{t_s}{2} \quad (6)$$

where $C_{PT}(t)$ and $C_{IT}(t)$ [dimensionless] are the normalized time-dependent concentrations measured in the effluent of the PT and the inert tracer, respectively. Finally, t_s [t] is the time required to inject the tracers.

Results and Discussion

Partition of Dyes in NAPL/Water Systems

The five fluorescent dyes (F, EY, RB, RWT, and SRB) were assessed as PTs of different polarities in four two-phase liquid systems made of 1) NAPL/water mixtures. The partitioning isotherms of the two-phase systems are shown in Supplementary Material S3. The partition coefficients of fluorescent dyes are summarized in Table 3. Their linearity (see the R²-values in Table 3) demonstrates constant partition values over a ppm-concentration range which facilitates partitioning determinations (Wise 1999; Wise et al. 1999). Some authors have demonstrated that PCE/dye (i.e., rhodamine WT, sulforhodamine, eosine) partition coefficients for the dyes were fit to linear isotherms in batch experiments (Ghanem et al. 2003). From a literature survey, the $\log K_{ow}$ values for EY and RB are close to those reported (see Table 1). However, the calculated $\log K_{ow}$ values for F, SRB, and RWT differ substantially

compared to the ones reported in the literature (Table 1), which systematically appear more hydrophilic. Unfortunately, little information is available about the conditions, such as pH, for these compounds with acid-base properties, in which the measurements were performed (Wang and Lien 1980).

Typical hydrophilic non-partitioning alcohols tracers used in PITT like ethanol, methanol, isopropanol, and 2-methyl-2-propanol have $\log K_{ow}$ -values ranging below -1 (Willson et al. 2000; Young et al. 1999). Longer carbon chains (C8 or C9) are used to obtain higher K_{nw} (Deeds et al. 2000). Yet, alcohol PTs have $\log K_{ow}$ -values ranging from 0.3 to 2.6, according to the same literature. In our study, the PT dyes display $\log K_{ow}$ -values ranging from -0.4 to 1.9, which is slightly narrower and shifted to lower values but quite similar to the PTs alcohols used in PITT. PT dyes display a higher affinity for the DNAPLs of COCs than for octanol, except for SRB which is relatively unaffected by the nature of the biphasic system. The PT affinity for DNAPLs increases significantly when small molecules are included in the COC mixture (e.g. PCE), as expected from the solubilization ability of the organic phase for organic compounds. For DNAPL/water systems, the $\log K_{nw}$ range from -0.4 to 1 for H/W and from 0 to 2.6 for M/W. However, higher partition constant values do not mean greater accuracy in assessing the NAPL saturation within an aquifer, because the retardation factor depends also on the NAPL saturation (equation 2 and 4). For example, for NAPL saturation of ~0.18%, PTs with $\log K_{nw}$ -values as high as two exhibited very poor recovery and difficulty in interpreting breakthrough curves compared to PTs with $\log K_{nw}$ ranging from 0.5 to 1.1 which only slightly underestimated NAPL saturations (Hartog et al. 2010; Ervin et al. 2011; Schaefer et al. 2016). When assessing NAPL saturation in a contaminated area, it is critical to inject a mixture of PTs with a wide range of partitioning properties.

Predictability of Partition Coefficients from Linear Free-Energy Relations

Selecting appropriate tracers for a given two-phase system under specific conditions requires a quantitative assessment of their partitioning behavior, which entails time-consuming and costly processes. Various researchers

have attempted to deduce the partition mechanisms of potential tracers from single and multi-parameter linear free-energy relations (LFERs) to make it easier to calculate partitioning properties (Kamlet et al. 1988; Marcus 1991; Thal et al. 2007). The free-energy of transfer of a series of compounds in a two-phase system between phases is considered to be linear in these models (Schwarzenbach et al. 2017):

$$\Delta_{12}G^i = a'\Delta_{34}G^i + b' \quad (7)$$

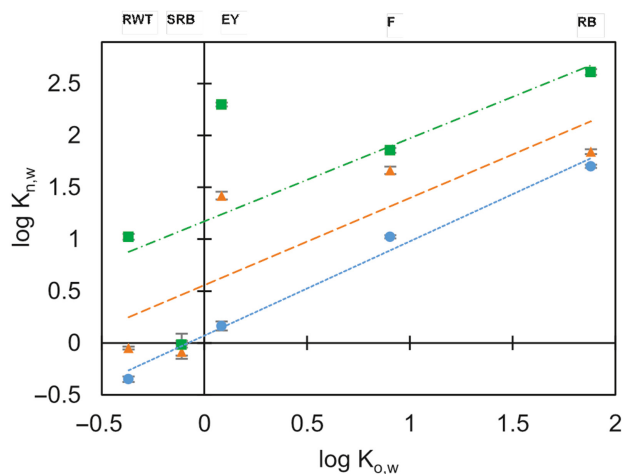
where $\Delta_{12}G^i$ and $\Delta_{34}G^i$ represents the free energy of the compound i from the two-phase system 1/2 to the 3/4 one, respectively. In addition, a' and b' are regression parameters. Equation 7 can then be written in terms of partition coefficients for aqueous two-phase systems where the octanol/water system is a reference:

$$\log K_{xw} = a \times \log K_{ow} + b \quad (8)$$

where a and b are specific parameters.

The predictability of the partition coefficient of the dyes among the H/W, T/W, and M/W systems ($\log K_{hw}$, $\log K_{tw}$, and $\log K_{mw}$) from $\log K_{ow}$ -values was compared. Results are shown in Figure 2. The scatter plot demonstrates a high level of predictability ($R^2=0.99$) of $\log K_{hw}$ from $\log K_{ow}$, even though the chemical structures of the fluorescent dyes differ.

This is assumed to result from a dehydrochlorination reaction of reactive COCs in T and M like PCE, whereas the HCBd is more inert (Schwarzenbach et al. 2017). Figure 2 shows more dispersed results for the predictability of $\log K_{tw}$ and $\log K_{mw}$ from $\log K_{ow}$, particularly for RWT, SRB, and EY fluorescent dyes. In this situation, not only can molecular interactions affect bulk organic phase changes, but more soluble organic compounds can alter the solvation properties of the aqueous phase (Kasnavia et al. 1999). As shown in Table 3, the pH of the aqueous solution in the two-phase systems decreased according to the order O/W > H/W > T/W > M/W from approximately 6 to 4. This pH change can strongly influence the abundance of PTs' acid-base species in equilibrium when the pH approaches pKa-values. As shown in Figure 2, the predictability (R^2 -values) of the LFERs decreases strongly from 0.99 to 0.48 for the DNAPL systems of higher complexity, resulting in larger pH-shifts to more acidic conditions. This predictability is completely correlated ($R^2 \cong 1$) to the pH shift. According to the pKa values of dyes (Table 1), their robustness toward pH changes from the reference O/W system decreases as follows: SRB >> RB > EY > RWT > F. F is especially sensitive to pH changes, given that the pH values vary between two pKa-values separated by 2.3 units, which strongly affects its partition constant. The 50% and 90% changes for the O/W system are expected based on the acid-base speciation for T/W and M/W, respectively. EY displays increasing hydrophobicity in T/W and M/W systems, as expected from the neutralization of its carboxylate moiety when pH approaches its pKa (Kasnavia et al. 1999; Batistela et al. 2011; Oba and Poulson 2012; Majek et al. 2014). In contrast, SRB and RB are both robust to pH changes



$$\log K_{nw} = a \times \log K_{ow} + b$$

Experimental data	System	$\log K_{nw}$	a	b	R^2
●	H,W	$\log K_{hw}$	0.91 ± 0.05	0.07 ± 0.05	0.989
▲	T,W	$\log K_{tw}$	0.84 ± 0.33	0.55 ± 0.33	0.660
■	M,W	$\log K_{mw}$	0.80 ± 0.48	1.17 ± 0.45	0.478

Figure 2. Logarithm of the N/W (Khw, Ktw, Kmw) partition constants vs. O/W (Kow) partition constants at 20°C.

and display contrasted affinities for the NAPLs. However, their absorption spectra differ by about 10 nm. Finally, the partition constant of SRB seems relatively unaffected by the nature of the NAPLs investigated here. This is not surprising given its hydrophilic character.

We have chosen RWT as a PT for later experiments because, it has a particular specificity for the complex mixture of NAPLs (M) despite pH changes. It is the only fluorescent dye we tested that possesses a hydrophilic character in contact with O, H, and T and a hydrophobic character in contact with M (see Table 3). In addition, its $\log K_{mw}$ value is best positioned for a good tracer recovery rate in comparison to field experiences (i.e., 0.5 to 1.1; Hartog et al. 2010).

Tracer Tests for Residual Saturation Estimation

The breakthrough curves for tracers revealed a delayed release of RWT vs. sodium chloride (see figures in Supplementary Material S4). The residual saturation of M was calculated using the method of moments (equation 4 through 7). The calculated retardation values were 1.12, 1.18, 1.16, and 1.09 for the flow rates of 1.0, 4.0, 10.0, and 40.0 mL/min, respectively. These results confirm the fact that the variation of the retardation factor with tracer injection flow rate is not significant (Mariner et al. 1999). The calculated retardation factors are (within our experiment accuracy) in the lower range limit of the recommended minimum retardation stated as important by various authors (Jin et al. 1997; Annable et al. 1998; Jalbert et al. 2003; Giraud 2018). It was suggested that retardation factors should range from 1.2 to 4.0, to provide sufficient separation from the conservative tracer breakthrough curve, while allowing reasonable PT

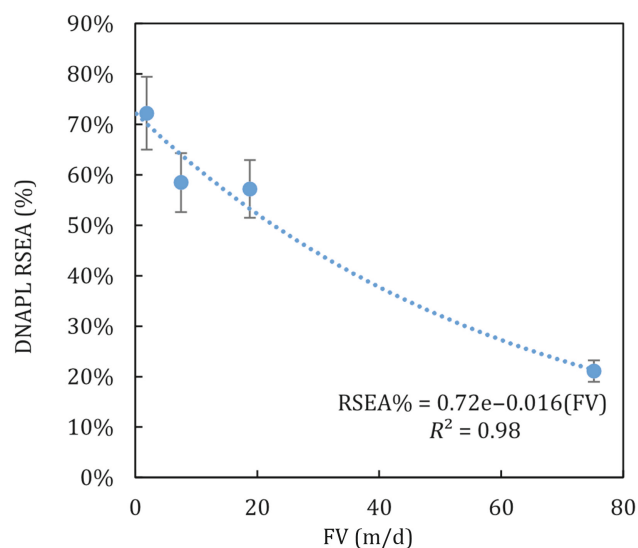


Figure 3. DNAPL residual saturation estimation accuracy (RSEA %) vs. tracer flow velocity (m/d).

mass recovery over the test duration (Jin et al. 1995). In the case where the adsorption on the mineral surfaces is not too high, the calculations of the residual saturation are more precise (Jin et al. 1995). For low residual NAPL saturations, the adsorption of tracers can take place on the natural organic material and potentially leads to an increase in the retardation factor (Jin et al. 1997). Field PITTs generally target R much lower than 4. Hartog et al. (2010) performed PITTs with R between 1.0 and 1.29. Istok et al. (2002), using alcohols, found retardation factors between 1.4 and 4, depending on the experimental conditions.

As shown in Figure 3, DNAPL RSEA is influenced by the tracer flow velocity. Decreasing the tracer flow velocity increases the contact time between the PT and the DNAPL, and consequently, the partition equilibrium approached. This allows us to estimate the DNAPL volume in the column more accurately. In addition, the higher water flow rate can increase the hydraulic dispersion (and decrease the local contact times) inside the column. The local velocity inside the column can also be slightly higher at the column walls compared to the velocity in porous media for higher flow rates. Furthermore, the decreasing RSEA may be explained by some observed migration of DNAPL droplets that occurs at high water velocities, resulting in a hydrophobic pool zones less swept by the tracer flow (Brooks et al. 2002; Enfield et al. 2005). Heterogeneity, macro-entrapped, high-saturation NAPL lenses, and pool morphology could significantly decrease the estimation of NAPL saturation (Dai et al. 2001; Fernández-García et al. 2002; Barth et al. 2003; Moreno-Barbero and Illangasekare 2006). Finally, PT mass transfer and equilibrium partitioning take longer to occur for NAPL droplets that are more interconnected.

Under controlled conditions in the laboratory, RWT in combination with sodium chloride underestimates the total residual saturation of M by about 25%. Nevertheless, this sensitivity experiment exposes a fitted exponential regression ($R^2=0.98$) working as a correlation function between the water velocity during the test and the RSEA on DNAPL (Figure 3).

Conclusion

We assessed five common fluorescent dyes as PTs, to estimate the residual saturation of NAPLs including eosin Y, fluorescein, sulforhodamine B, rhodamine B, and rhodamine WT. The three DNAPLs we considered had increasing complexity from models (artificial mixtures of a single or multiple COCs) to a real historical contamination (a mixture of COCs) and used octanol as a reference. The pH of the aqueous phase in contact with the DNAPLs decreased as the number of COCs in the mixture increased.

Partition equilibria were constant within the ppm-concentration range and easily quantified. However, the partition constants associated with fluorescein, rhodamine WT, and eosin Y were especially sensitive to pH changes in the 4 to 6 range, which hinder their use. Rhodamine B and sulforhodamine B are robust regarding the pH-range of natural water and display contrasted partition constants matching with PITT applications. Deviations observed from LFERs between DNAPL/water and octanol/water were also strongly correlated to pH changes.

Finally, the influence of water velocity (0 to 80 m/d) on the residual NAPL saturation estimation was studied in PT tests carried out in a column packed with 1 mm glass beads. Glass beads were used to isolate the effect of tracer injection flow rate on the estimation of the DNAPL residual saturation given potential effects on the retardation factor resulting from tracer sorption on soil organic matter. The analysis of the breakthrough curves generally underestimated the amount of the residual contaminant by a minimum of 25% at least, although increasing exponentially with the water velocity. This behavior may be related to the exponential behavior of tracer dispersivity with velocity (or Péclet number). Since we know how the tracer injection velocity can influence the estimation of the residual contaminant saturation, the fitted exponential function could be used as a correction formula to overcome the method's inaccuracy.

Acknowledgments

The authors would like to thank the French Environment and Energy Management Agency (ADEME) and the BRGM/DEPA for providing the Ph.D. grant for Sofia Visitation. We gratefully acknowledge financial support provided to the FAMOUS project by ADEME. The authors are also thankful for financial support provided to the PIVOTS project by the “Région Centre – Val de Loire”, the European Regional Development Fund (ERDF), and the “Région Nouvelle Aquitaine”.

Supporting Information

Additional Supporting Information may be found in the online version of this article. Supporting Information is generally not peer reviewed.

Supplementary Material S1. $\log K_{ow}$ Values of fluorescent dyes.

Supplementary Material S2. pH Values.

Supplementary Material S3. Fluorescent dyes K_{ow} in different systems. a. O/W b. H/W c. T/W and d. M/W.

Supplementary Material S4. Breakthrough curves PT experiences in porous media.

References

- Annable, M.D., J.W. Jawitz, P.S.C. Rao, D.P. Dai, H. Kim, and A.L. Wood. 1998. Field evaluation of interfacial and partitioning tracers for characterization of effective NAPL-water contact areas. *Ground Water* 36, no. 3: 495–502.
- Aparecida de Melo, M., and de Holleben, C. A. A., ed. 2001. Using tracers to characterize petroleum reservoirs: Application to Campopolis Field, Brazil. Paper presented at All Days of SPE Latin America and Caribbean Petroleum Engineering Conference. SPE-69474-MS.
- Banerjee, S. 1984. Solubility of organic mixtures in water. *Environmental Science & Technology* 18, no. 8: 587–591. <https://doi.org/10.1021/es00126a004>
- Barth, G.R., T.H. Illangasekare, and H. Rajaram. 2003. The effect of entrapped nonaqueous phase liquids on tracer transport in heterogeneous porous media: Laboratory experiments at the intermediate scale. *Journal of Contaminant Hydrology* 67, no. 1: 247–268.
- Batistela, V.R., D.S. Pellosi, F.D. De Souza, W.F. Da Costa, S.M. De Oliveira Santin, V.R. De Souza, and N. Hioka. 2011. pKa determinations of xanthene derivatives in aqueous solutions by multivariate analysis applied to UV-vis spectrophotometric data. *Spectrochimica Acta. Part A: Molecular and Biomolecular Spectroscopy* 79, no. 5: 889–897. <https://doi.org/10.1016/j.saa.2011.03.027>
- Brooks, M.C., M.D. Annable, P.S.C. Rao, K. Hatfield, J.W. Jawitz, W.R. Wise, and C.G. Enfield. 2002. Controlled release, blind tests of DNAPL characterization using partitioning tracers. *Journal of Contaminant Hydrology* 59, no. 3–4: 187–210. [https://doi.org/10.1016/S0169-7722\(02\)00057-8](https://doi.org/10.1016/S0169-7722(02)00057-8)
- Cazaux, D., S. Colombano, A. Dumestre, A., Joubert, and G. Lecuelle. 2014. Optimized physical recovery of DNAPL using upwelling technique and geostatistical analysis at large field scale. Ninth International Conference on Remediation of Chlorinated and Recalcitrant Compounds, Monterey, United States.
- Chambers, L., D. Goody, and A. Binley. 2019. Use and application of cfc-11, cfc-12, cfc-113 and sf6 as environmental tracers of groundwater residence time: A review. *Geoscience Frontiers* 10, no. 5: 1643–1652.
- ChemicalBook. 2022. ChemicalBook—Chemical Search Engine. https://www.chemicalbook.com/ProductIndex_EN.aspx (accessed January 26, 2022).
- Cochennec, M., H. Davarzani, S. Colombano, I. Ignatiadis, Y. Davit, and M. Quintard. 2022. Impact of gravity and inertia on stable displacements of DNAPL in highly permeable porous media. *Advances in Water Resources* 162: 104139. <https://doi.org/10.1016/j.advwatres.2022.104139>
- Colombano, S., H. Davarzani, E.D. van Hullebusch, D. Huguenot, D. Guyonnet, J. Deparis, and I. Ignatiadis. 2021. Permittivity and electrical resistivity measurements and estimations during the recovery of DNAPL in saturated porous media: 2D tank experiments. *Journal of Applied Geophysics* 191: 104359. <https://doi.org/10.1016/j.jappgeo.2021.104359>
- Colombano, S., H. Davarzani, E.D. van Hullebusch, D. Huguenot, D. Guyonnet, J. Deparis, and I. Ignatiadis. 2020. Thermal and chemical enhanced recovery of heavy chlorinated organic compounds in saturated porous media: 1D cell drainage-imbibition experiments. *Science of the Total Environment* 706: 135758. <https://doi.org/10.1016/j.scitotenv.2019.135758>
- Cook, P.G., D.K. Solomon, L.N. Plummer, E. Busenberg, and S.L. Schiff. 1995. Chlorofluorocarbons as tracers of groundwater transport processes in a shallow, silty sand aquifer. *Water Resources Research* 31, no. 3: 425–434.
- Cumming, H., and C. Rücker. 2017. Octanol-water partition coefficient measurement by a simple 1H NMR method. *ACS Omega* 2, no. 9: 6244–6249. <https://doi.org/10.1021/acsomega.7b01102>
- Dai, D., F.T. Barranco, and T.H. Illangasekare. 2001. Partitioning and interfacial tracers for differentiating napl entrapment configuration: Column-scale investigation. *Environmental Science & Technology* 35, no. 24: 4894–4899. <https://doi.org/10.1021/es010745k>
- Dearden, J.C., and G.M. Bresnen. 1988. Review: The measurement of partition coefficients. *Quantitative Structure-Activity Relationships* 7: 133–144.
- Deeds, N.E., D.C. McKinney, and G.A. Pope. 2000. Laboratory characterization of non-aqueous phase liquid/tracer interaction in support of a vadose zone partitioning interwell tracer test. *Journal of Contaminant Hydrology* 41, no. 1: 193–204.
- DiFilippo, E.L., and M.L. Brusseau. 2008. Relationship between mass-flux reduction and source-zone mass removal: Analysis of field data. *Journal of Contaminant Hydrology* 98, no. 1–2: 22–35. <https://doi.org/10.1016/j.jconhyd.2008.02.004>
- Dörfliger, N. 2010. Guide méthodologique: Les outils de l'hydrogéologie karstique pour la caractérisation de la structure et du fonctionnement des systèmes karstiques et l'évaluation de leur ressource. Orleans.
- Enfield, C.G., A.L. Wood, F.P. Espinoza, M.C. Brooks, M. Annable, and P. Rao. 2005. Design of aquifer remediation systems: (1) describing hydraulic structure and NAPL architecture using tracers. *Journal of Contaminant Hydrology* 81, no. 1: 125–147. <https://www.sciencedirect.com/science/article/pii/S0169772205001427>
- Ervin, R.E., A. Boroumand, L.M. Abriola, and C.A. Ramsburg. 2011. Kinetic limitations on tracer partitioning in ganglia dominated source zones. *Journal of Contaminant Hydrology* 126, no. 3–4: 195–207. <https://doi.org/10.1016/j.jconhyd.2011.07.006>
- Falta, R.W., P. Suresh Rao, and N. Basu. 2005. Assessing the impacts of partial mass depletion in DNAPL source zones: I. Analytical modeling of source strength functions and plume response. *Journal of Contaminant Hydrology* 78, no. 4: 259–280. <https://doi.org/10.1016/j.jconhyd.2005.05.010>
- Fernández-García, D., X. Sánchez-Vila, and T.H. Illangasekare. 2002. Convergent-flow tracer tests in heterogeneous media: combined experimental-numerical analysis for determination of equivalent transport parameters. *Journal of Contaminant Hydrology* 57, no. 1: 129–145. <https://www.sciencedirect.com/science/article/pii/S0169772201002145>
- Ghanem, A., T.S. Soerens, M.M. Adel, and G.J. Thoma. 2003. Investigation of fluorescent dyes as partitioning tracers for subsurface nonaqueous phase liquid (napl) characterization. *Journal of Environmental Engineering* 129, no. 8: 740–744.
- Giraud, Q. 2018. Modélisation du devenir de contaminants organiques dans le sol. Aix-Marseille Université.
- Harris, M.F., and J.L. Logan. 2014. Determination of log Kow values for four drugs. *Journal of Chemical Education* 91, no. 6: 915–918. <https://doi.org/10.1021/ed400655b>
- Hartog, N., J. Cho, B.L. Parker, and M.D. Annable. 2010. Characterization of a heterogeneous DNAPL source zone in the Borden aquifer using partitioning and interfacial tracers: Residual morphologies and background sorption. *Journal of Contaminant Hydrology* 115, no. 1–4: 79–89. <https://doi.org/10.1016/j.jconhyd.2010.04.004>
- Interstate Technology and Regulatory Council. 2005. Overview of In Situ Bioremediation of Chlorinated Ethene DNAPL Source

- Zones. Washington, DC. www.itrcweb.org (accessed October 22, 2019).
- Istok, J.D., J.A. Field, M.H. Schroth, B.M. Davis, and V. Dwarkanath. 2002. Single-well “push-pull” partitioning tracer test for NAPL detection in the subsurface. *Environmental Science & Technology* 36, no. 12: 2708–2716. <https://doi.org/10.1021/es015624z>
- Jalbert, M., J.H. Dane, and L. Bahaminyakamwe. 2003. Influence of porous medium and NAPL distribution heterogeneities on partitioning inter-well tracer tests: A laboratory investigation. *Journal of Hydrology* 272, no. 1–4: 79–94. [https://doi.org/10.1016/S0022-1694\(02\)00256-1](https://doi.org/10.1016/S0022-1694(02)00256-1)
- Jin, M., G.W. Butler, R.E. Jackson, P.E. Mariner, J.F. Pickens, G.A. Pope, C.L. Brown, and D.C. McKinney. 1997. Sensitivity models and design protocol for partitioning tracer tests in alluvial aquifers. *Ground Water* 35: 964–972. <https://doi.org/10.1111/j.1745-6584.1997.tb00168.x>
- Jin, M., M. Delshad, V. Dwarkanath, D.C. McKinney, G.A. Pope, K. Sepehrnoori, C.E. Tilburg, and R.E. Jackson. 1995. Partitioning tracer test for detection, estimation, and remediation performance assessment of subsurface nonaqueous phase liquids. *Water Resources Research* 31, no. 5: 1201–1211. <https://doi.org/10.1029/95WR00174>
- Kamlet, M.J., M.H. Abraham, P.W. Carr, R.M. Doherty, and R.W. Taft. 1988. Solute–solvent interactions in chemistry and biology. Part 7. An analysis of mobile phase effects on high pressure liquid chromatography capacity factors and relationships of the latter with octanol–water partition coefficients. *Journal of the Chemical Society, Perkin Transactions 2*, no. 12: 2087–2092. <https://doi.org/10.1039/P29880002087>
- Kasnavia, T., D. Vu, and D.A. Sabatini. 1999. Fluorescent dye and media properties affecting sorption and tracer selection. *Ground Water Monitoring and Remediation* 37, no. 3: 376–381.
- Khan, S.M., S.-S. Rhee, and J. Park. 2008. The interference of organic matter in the characterization of aquifers contaminated with LNAPLs by partitioning tracer method. *Journal of the Korean Geotechnical Society* 24, no. 9: 13–21.
- Khmelnitskiy, V., N. AlJabri, and V. Solovyeva. 2022. Fluorescent based tracers for oil and gas downhole applications: Between conventional and innovative approaches. *Engineering Proceedings* 19, no. 1: 1–6.
- Klonis, N., and W.H. Sawyer. 1996. Spectral properties of the prototropic forms of fluorescein in aqueous solution. *Journal of Fluorescence* 6, no. 3: 147–157. <https://doi.org/10.1007/BF00732054>
- Król, A., M. Gajec, and E. Kukulska-Zajac. 2021. Uranine as a tracer in the oil and gas industry: Determination in formation waters with high-performance liquid chromatography. *Water* 13, no. 21: 3082.
- Leibundgut, C., P. Maloszewski, and C. Külls. 2009. *Tracers in Hydrology*. West Sussex: Office (John Wiley).
- Mackay, D.M., and J.A. Cherry. 1989. Groundwater contamination: pump-and-treat remediation. *Environmental Science & Technology* 23, no. 6: 630–636. <https://doi.org/10.1021/es00064a001>
- Maire, J., and N. Fatin-Rouge. 2017. Surfactant foam flushing for in situ removal of DNAPLs in shallow soils. *Journal of Hazardous Materials* 321: 247–255. <https://doi.org/10.1016/j.jhazmat.2016.09.017>
- Majek, M., F. Filace, and A.J. Von Wangelin. 2014. On the mechanism of photocatalytic reactions with eosin y. *Beilstein Journal of Organic Chemistry* 10: 981–989. <https://doi.org/10.3762/bjoc.10.97>
- Marcus, Y. 1991. Linear solvation energy relationships. Correlation and prediction of the distribution of organic solutes between water and immiscible organic solvents. *Journal of Physical Chemistry* 95, no. 22: 8886–8891. <https://doi.org/10.1021/J100175A086>
- Mariner, P.E., M. Jin, J.E. Studer, and G.A. Pope. 1999. The first vadose zone partitioning interwell tracer test for nonaqueous phase liquid and water residual. *Environmental Science & Technology* 33, no. 16: 2825–2828. <https://doi.org/10.1021/es9901720>
- McDade, J.M., T.M. McGuire, and C.J. Newell. 2005. Analysis of DNAPL source-depletion costs at 36 field sites. *Remediation* 15, no. 2: 9–18. <https://doi.org/10.1002/rem.20039>
- McGuire, T.M., J.M. McDade, and C.J. Newell. 2006. Performance of DNAPL source depletion technologies at 59 chlorinated solvent-impacted sites. *Ground Water Monitoring and Remediation* 26, no. 1: 73–84. <https://doi.org/10.1111/j.1745-6592.2006.00054.x>
- Montgomery, J.H. 2007. *Groundwater Chemicals Desk Reference* (4th ed.). CRC Press. <https://doi.org/10.1201/9781420009132>
- Moreno-Barbero, E., and T.H. Illangasekare. 2006. Influence of dense nonaqueous phase liquid pool morphology on the performance of partitioning tracer tests: Evaluation of the equilibrium assumption. *Water Resources Research* 42, no. 4: W04408.
- MTES. 2018. Base des données BASOL. 2019. <https://basol.developpement-durable.gouv.fr/> (accessed December 27, 2019).
- Muller, K.A., and C.A. Ramsburg. 2018. Influence of nonwetting phase saturation on dispersivity in laboratory-scale sandy porous media. *Environmental Engineering Science* 35, no. 10: 1062–1074. <https://doi.org/10.1089/ees.2017.0444>
- NIEHS. 2015. Chlorinated organics – Information page. http://tools.niehs.nih.gov/srp/research/research4_s3_s4.cfm (accessed October 22, 2019).
- Oba, Y., and S.R. Poulson. 2012. Octanol-water partition coefficients (Kow) vs. Ph for fluorescent dye tracers (fluorescein, eosin y), and implications for hydrologic tracer tests. *Geochemical Journal* 46, no. 6: 517–520. <https://doi.org/10.2343/geochemj.2.0226>
- OECD. 1995. *Test No. 107: Partition Coefficient (n-octanol/water): Shake Flask Method*. OECD Guidelines for the Testing of Chemicals, Section 1, Éditions OCDE, Paris. <https://doi.org/10.1787/9789264069626-en>
- Ohms, D., J. McLeod, C.J. Graff, H. Frampton, J.C. Morgan, S. Cheung, and K.T. Chang. 2010. Incremental-oil success from waterflood sweep improvement in Alaska. *SPE Production & Operations* 25, no. 3: 247–254.
- Philippe, N., H. Davarzani, S. Colombano, M. Dierick, P.Y. Klein, and M. Marcoux. 2020. Experimental study of the temperature effect on two-phase flow properties in highly permeable porous media: Application to the remediation of dense nonaqueous phase liquids (DNAPLs) in polluted soil. *Advances in Water Resources* 146: 103783. <https://doi.org/10.1016/j.advwatres.2020.103783>
- Philippe, N., H. Davarzani, S. Colombano, M. Dierick, P.Y. Klein, and M. Marcoux. 2021. Experimental study of thermally enhanced recovery of high-viscosity DNAPL in saturated porous media under non-isothermal conditions. *Journal of Contaminant Hydrology* 243: 103861. <https://doi.org/10.1016/j.jconhyd.2021.103861>
- Rathfelder, K.M., L.M. Abriola, M.A. Singletary, and K.D. Pennell. 2003. Influence of surfactant-facilitated interfacial tension reduction on chlorinated solvent migration in porous media: Observations and numerical simulation. *Journal of Contaminant Hydrology* 64, no. 3–4: 227–252. [https://doi.org/10.1016/S0169-7722\(02\)00205-X](https://doi.org/10.1016/S0169-7722(02)00205-X)
- Salman, M., and K. Kostarelos. 2019. An expression for irregularly distributed hydrocarbon volume using exponential decay method. *Environmental Geotechnics* 8, no. 8: 539–546. <https://doi.org/10.1680/jenge.18.00062>
- Schaefer, C.E., E.B. White, G.M. Lavorgna, and M.D. Annable. 2016. Dense nonaqueous-phase liquid architecture in fractured bedrock: Implications for treatment and plume longevity. *Environmental Science and Technology* 50, no. 1: 207–213. <https://doi.org/10.1021/acs.est.5b04150>

- Schwarzenbach, R.P., P.M. Gschwend, and D.M. Imboden. 2017. *Environmental Organic Chemistry*, 3rd ed. NJ: John Wiley and Sons Inc, New York.
- Simon, M.A., and M.L. Brusseau. 2007. Analysis of a gas-phase partitioning tracer test conducted in an unsaturated fractured-clay formation. *Journal of Contaminant Hydrology* 90, no. 3: 146–158.
- Thal, A.E., R.C. Knox, and D.A. Sabatini. 2007. Estimating partition coefficients of tracers. *Ground Water Monitoring and Remediation* 27, no. 4: 135–142. <https://doi.org/10.1111/j.1745-6592.2007.00165.x>
- Vasudevan, D., R.L. Fimmen, and A.B. Francisco. 2001. Tracer-grade rhodamine wt: Structure of constituent isomers and their sorption behavior. *Environmental Science & Technology* 35: 4089–4096.
- Wang, P.-H., and E.J. Lien. 1980. Effects of different buffer species on partition coefficients of drugs used in quantitative structure-activity relationships. *Journal of Pharmaceutical Sciences* 69, no. 6: 662–668. <https://www.sciencedirect.com/science/article/pii/S0022354915432265>
- Werner, D., H.K. Karapanagioti, and P. Höhener. 2009. Diffusive partitioning tracer test for the quantification of nonaqueous phase liquid (NAPL) in the vadose zone: Performance evaluation for heterogeneous napl distribution. *Journal of Contaminant Hydrology* 108, no. 1: 54–63.
- Werner, D., and P. Höhener. 2002. Diffusive partitioning tracer test for nonaqueous phase liquid (NAPL) detection in the vadose zone. *Environmental Science & Technology* 36: 1592–1599.
- Willson, C.S., O. Pau, J.A. Pedit, and C.T. Miller. 2000. Mass transfer rate limitation effects on partitioning tracer tests. *Journal of Contaminant Hydrology* 45, no. 1–2: 79–97. [https://doi.org/10.1016/S0169-7722\(00\)00120-0](https://doi.org/10.1016/S0169-7722(00)00120-0)
- Wilson, R.D., and D.M. Mackay. 1995. Direct detection of residual nonaqueous phase liquid in the saturated zone using SF6 as a partitioning tracer. *Environmental Science & Technology* 29, no. 5: 1255–1258.
- Wise, W.R. 1999. NAPL characterization via partitioning tracer tests: Quantifying effects of partitioning nonlinearities. *Journal of Contaminant Hydrology* 36, no. 1: 167–183.
- Wise, W.R., D. Dai, E.A. Fitzpatrick, L.W. Evans, P.C. Rao, and M.D. Annable. 1999. Non-aqueous phase liquid characterization via partitioning tracer tests: A modified langmuir relation to describe partitioning nonlinearities. *Journal of Contaminant Hydrology* 36, no. 1: 153–165.
- Young, C.M., R.E. Jackson, M. Jin, J.T. Londergan, P.E. Mariner, G.A. Pope, F.J. Anderson, and T. Houk. 1999. Characterization of a TCE DNAPL zone in alluvium by partitioning tracers. *Groundwater Monitoring & Remediation* 19: 84–94. <https://doi.org/10.1111/j.1745-6592.1999.tb00190.x>

Biographical Sketches

Sofia Visitacion-Carrillo is at French Geological Survey (BRGM), Orléans, France; Institut de Chimie des Milieux et Matériaux de Poitiers (IC2MP), University of Poitiers, CNRS, F-86073 Poitiers, France; Agence de la transition écologique (ADEME), Angers, France.

Stéfan Colombano, Ph.D., is at French Geological Survey (BRGM), Orléans, France.

Nicolas Fatin-Rouge, Ph.D., is at Institut de Chimie des Milieux et Matériaux de Poitiers (IC2MP), University of Poitiers, CNRS, F-86073 Poitiers, France.

Dorian Davarzani, Ph.D., corresponding author, is at French Geological Survey (BRGM), Orléans, France; +33 (0)2 38 64 33 52; d.davarzani@brgm.fr